Efficiency of non-linear frequency conversion of double-scale pico-femtosecond pulses of passively mode-locked fiber laser

Sergey V. Smirnov,[*] Sergey M. Kobtsev, and Sergey V. Kukarin

Division of Laser Physics and Innovative Technologies, Novosibirsk State University, 630090, Novosibirsk, Russia
[*]*smirnov@lab.nsu.ru*

Abstract: For the first time we report the results of both numerical simulation and experimental observation of second-harmonic generation as an example of non-linear frequency conversion of pulses generated by passively mode-locked fiber master oscillator in different regimes including conventional (stable) and double-scale (partially coherent and noise-like) ones. We show that non-linear frequency conversion efficiency of double-scale pulses is slightly higher than that of conventional picosecond laser pulses with the same energy and duration despite strong phase fluctuations of double-scale pulses.

OCIS codes: (140.4050) Mode-locked lasers; (140.3510) Lasers, fiber; (140.7090) Ultrafast lasers; (190.2620) Harmonic generation and mixing.

References and links

1. V. J. Matsas, T. P. Newson, D. J. Richardson, and D. N. Payne, "Self-starting, passively mode-locked fibre ring soliton laser exploiting non-linear polarisation rotation," Electron. Lett. **28**(15), 1391–1393 (1992).
2. F. Ilday, J. Buckley, L. Kuznetsova, and F. Wise, "Generation of 36-femtosecond pulses from a ytterbium fiber laser," Opt. Express **11**(26), 3550–3554 (2003).
3. F. W. Wise, A. Chong, and W. H. Renninger, "High-energy femtosecond fiber lasers based on pulse propagation at normal dispersion," Laser Photonics Rev. **2**(1–2), 58–73 (2008).
4. S. Kobtsev, S. Kukarin, and Y. Fedotov, "Ultra-low repetition rate mode-locked fiber laser with high-energy pulses," Opt. Express **16**(26), 21936–21941 (2008).
5. P. Grelu and N. Akhmediev, "Dissipative solitons for mode-locked lasers," Nat. Photonics **6**(2), 84–92 (2012).
6. L. M. Zhao, D. Y. Tang, T. H. Cheng, and C. Lu, "Nanosecond square pulse generation in fiber lasers with normal dispersion," Opt. Commun. **272**(2), 431–434 (2007).
7. B. Ortaç, A. Hideur, M. Brunel, C. Chédot, J. Limpert, A. Tünnermann, and F. Ö. Ilday, "Generation of parabolic bound pulses from a Yb-fiber laser," Opt. Express **14**(13), 6075–6083 (2006).
8. J. M. Soto-Crespo, P. Grelu, N. Akhmediev, and N. Devine, "Soliton complexes in dissipative systems: vibrating, shaking, and mixed soliton pairs," Phys. Rev. E Stat. Nonlinear Soft Matter Phys. **75**(1), 016613 (2007).
9. W. H. Renninger, A. Chong, and F. W. Wise, "Pulse shaping and evolution in normal-dispersion mode-locked fiber lasers," IEEE J. Sel. Top. Quantum Electron. **18**(1), 389–398 (2012).
10. P. Grelu and J. M. Soto-Crespo, "Temporal soliton "molecules" in mode-locked lasers: collisions, pulsations, and vibrations," Lect. Notes Phys. **751**, 137–173 (2008).
11. S. Chouli and P. Grelu, "Rains of solitons in a fiber laser," Opt. Express **17**(14), 11776–11781 (2009).
12. A. Komarov, H. Leblond, and F. Sanchez, "Multistability and hysteresis phenomena in passively mode-locked fiber lasers," Phys. Rev. A **71**(5), 053809 (2005).
13. S. Kobtsev, S. Kukarin, S. Smirnov, S. Turitsyn, and A. Latkin, "Generation of double-scale femto/pico-second optical lumps in mode-locked fiber lasers," Opt. Express **17**(23), 20707–20713 (2009).
14. S. Smirnov, S. Kobtsev, S. Kukarin, and A. Ivanenko, "Three key regimes of single pulse generation per round trip of all-normal-dispersion fiber lasers mode-locked with nonlinear polarization rotation," Opt. Express **20**(24), 27447–27453 (2012).
15. M. Horowitz, Y. Barad, and Y. Silberberg, "Noiselike pulses with a broadband spectrum generated from an erbium-doped fiber laser," Opt. Lett. **22**(11), 799–801 (1997).
16. L. M. Zhao, D. Y. Tang, J. Wu, X. Q. Fu, and S. C. Wen, "Noise-like pulse in a gain-guided soliton fiber laser," Opt. Express **15**(5), 2145–2150 (2007).
17. D. Lei, H. Yang, H. Dong, S. Wen, H. Xu, and J. Zhang, "Effect of birefringence on the bandwidth of noise-like pulse in an erbium-doped fiber laser," J. Mod. Opt. **56**(4), 572–576 (2009).

#199337 - $15.00 USD Received 14 Oct 2013; revised 6 Dec 2013; accepted 3 Jan 2014; published 10 Jan 2014

18. Q. Wang, T. Chen, M. Li, B. Zhang, Y. Lu, and K. P. Chen, "All-fiber ultrafast thulium-doped fiber ring laser with dissipative soliton and noise-like output in normal dispersion by single-wall carbon nanotubes," Appl. Phys. Lett. **103**(1), 011103 (2013).
19. L. M. Zhao and D. Y. Tang, "Generation of 15-nJ bunched noise-like pulses with 93-nm bandwidth in an erbium-doped fiber ring laser," Appl. Phys. B **83**(4), 553–557 (2006).
20. D. Y. Tang, L. M. Zhao, and B. Zhao, "Soliton collapse and bunched noise-like pulse generation in a passively mode-locked fiber ring laser," Opt. Express **13**(7), 2289–2294 (2005).
21. S. M. Kobtsev and S. V. Smirnov, "Fiber lasers mode-locked due to nonlinear polarization evolution: golden mean of cavity length," Laser Phys. **21**(2), 272–276 (2011).
22. I. A. Yarutkina, O. V. Shtyrina, M. P. Fedoruk, and S. K. Turitsyn, "Numerical modeling of fiber lasers with long and ultra-long ring cavity," Opt. Express **21**(10), 12942–12950 (2013).
23. Y. Takushima, K. Yasunaka, Y. Ozeki, and K. Kikuchi, "87 nm bandwidth noise-like pulse generation from erbium-doped fibre laser," Electron. Lett. **41**(7), 399–400 (2005).
24. J. C. Hernandez-Garcia, O. Pottiez, and J. M. Estudillo-Ayala, "Supercontinuum generation in a standard fiber pumped by noise-like pulses from a figure-eight fiber laser," Laser Phys. **22**(1), 221–226 (2012).
25. L. Wang, X. Liu, Y. Gong, D. Mao, and L. Duan, "Observations of four types of pulses in a fiber laser with large net-normal dispersion," Opt. Express **19**(8), 7616–7624 (2011).
26. S. M. Kobtsev, S. V. Kukarin, and S. V. Smirnov, "All-fiber high-energy supercontinuum pulse generator," Laser Phys. **20**(2), 375–378 (2010).
27. M. L. Dennis, M. A. Putnam, J. U. Kang, T.-E. Tsai, I. N. Duling III, and E. J. Friebele, "Grating sensor array demodulation by use of a passively mode-locked fiber laser," Opt. Lett. **22**(17), 1362–1364 (1997).
28. S. M. Kobtsev and S. V. Smirnov, "Influence of noise amplification on generation of regular short pulse trains in optical fibre pumped by intensity-modulated CW radiation," Opt. Express **16**(10), 7428–7434 (2008).
29. V. G. Dmitriev, L. V. Tarasov, *Applied Nonlinear Optics* [in Russian] (M., Radio i svyaz', 1982).
30. S. Martin-Lopez, A. Carrasco-Sanz, P. Corredera, L. Abrardi, M. L. Hernanz, and M. Gonzalez-Herraez, "Experimental investigation of the effect of pump incoherence on nonlinear pump spectral broadening and continuous-wave supercontinuum generation," Opt. Lett. **31**(23), 3477–3479 (2006).
31. F. Vanholsbeeck, S. Martin-Lopez, M. González-Herráez, and S. Coen, "The role of pump incoherence in continuous-wave supercontinuum generation," Opt. Express **13**(17), 6615–6625 (2005).
32. S. M. Kobtsev and S. V. Smirnov, "Modelling of high-power supercontinuum generation in highly nonlinear, dispersion shifted fibers at CW pump," Opt. Express **13**(18), 6912–6918 (2005).
33. G. P. Agrawal, *Nonlinear Fiber Optics*, 3rd ed. (Academic, 2001).

1. Introduction

Fiber lasers mode-locked due to non-linear polarization evolution (NPE) effect [1] are known as a convenient and efficient tool to produce ultra-short optical pulses with scalable pulse duration and energy [2–4]. These lasers operate in a diversity of generation regimes [5] and are capable to generate pulses of different shape [6–9]. In addition to conventional single pulses at fundamental repetition rate, NPE-lasers may produce complex soliton structures [8,10], soliton rains [11], and regular pulse trains at frequencies being multiple of fundamental one [12]. Even among single-pulse generation regimes (i.e. when only one pulse or wave-packet (bunch) of sub-pulses is produced per cavity round-trip time) one can distinguish two different types of lasing regimes: conventional picosecond-long pulses with smooth envelope and phase and double-scale pico-femtosecond pulses with complex inner structure [13]. In the latter regime laser produces picosecond-long wave-packets comprising intensity fluctuations or even a stochastic sequence of femtosecond sub-pulses [13]. Integral parameters of the entire wave packet, such as energy and duration, fluctuate around their average values within a range from several up to dozens per cent from one wave-packet to another. Intensity fluctuations inside single wave-packets may also vary from relatively small values up to the peak intensity of the wave-packet. In the case of strong intensity fluctuation inside the wave-packet, this lasing regime is usually referred to as noise-like generation. Another case of relatively weak fluctuations of intensity and phase inside the wave-packet was reported in our previous study [14] and named "intermediate lasing regime" since it has transient properties between conventional and noise-like laser pulses. In this work we discuss both intermediate and noise-like pulses and for brevity we will call them double-scale pulses. Generation of double-scale pulses (usually picosecond pulses with strong intra-pulse intensity fluctuations, i.e. femtosecond noise-like oscillations) has been reported up to date by numerous authors (see e.g [13–22].). Moreover, generation regimes featuring double-scale

#199337 - $15.00 USD Received 14 Oct 2013; revised 6 Dec 2013; accepted 3 Jan 2014; published 10 Jan 2014

pulses may be most likely found in long and ultra-long high-energy lasers [21,22], what makes them particularly interesting for applications. However, applicability of such pulses was until now the subject of only a few papers considering mainly super-continuum generation [23–26] and optical sensing [27]. The key qualitative difference between conventional and double-scale pulses is related to their different pulse-to-pulse coherence and phase fluctuation level [14]. From the viewpoint of laser applications, radiation incoherence may play either negative [28,29] or positive role [30–32] depending on application. In this paper, we investigate for the first time applicability of double-scale pulses obtained from all-normal dispersion fiber lasers mode-locked via NPE for non-linear frequency conversion using second harmonic generation (SHG) in a crystal with spectral acceptance bandwidth exceeding the pulse spectrum width, as one of the most basic examples.

In general, efficiency of non-linear transformation of ultra-short (femtosecond) pulses is relatively high. Nevertheless, this efficiency in the case of long trains of ultra-short sub-pulses is not known in advance since the energy of the pulse is distributed over a large number of femtosecond sub-pulses with strong phase fluctuations. Therefore, it's interesting to compare SHG efficiency for double-scale and conventional ("single-scale") laser pulses.

2. Numerical model

In order to investigate the influence of partial pulse coherence on SHG efficiency, we start with numerical simulations of a laser similar to those used in our previous experiments [13,14]. Thus, we consider a fiber ring cavity (see Fig. 1(a)) formed by a 6-m long active ytterbium fiber and a 4-m long passive fiber. For control of the polarization state in the optical train, two fiber-based polarization controllers PC1 and PC2 are employed. All optical fibers in this layout have normal dispersion within the working spectral range of the laser. As it was done earlier [13,14] we simulate the laser using a standard approach based on the system of modified non-linear Schrödinger Eqs. (1) and (2) [33]:

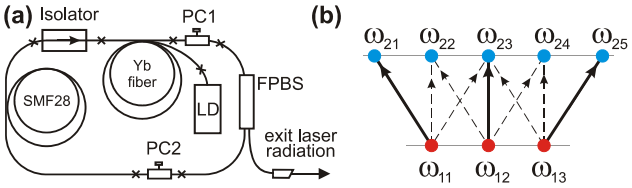

Fig. 1. (a) Laser layout: PC — polarization controller, FPBS — fiber polarization beam splitter, LD — pump laser diode. (b) Schematic of SHG processes for $N = 3$ modes.

$$\frac{\partial A_x}{\partial z} = i\gamma\left\{\left|A_x\right|^2 A_x + \frac{2}{3}\left|A_y\right|^2 A_x + \frac{1}{3}A_y^2 A_x^*\right\} + \frac{g_0/2}{1+E/\left(P_{sat}\cdot\tau\right)}A_x - \frac{i}{2}\beta_2\cdot\frac{\partial^2 A_x}{\partial t^2} \quad (1)$$

$$\frac{\partial A_y}{\partial z} = i\gamma\left\{\left|A_y\right|^2 A_y + \frac{2}{3}\left|A_x\right|^2 A_y + \frac{1}{3}A_x^2 A_y^*\right\} + \frac{g_0/2}{1+E/\left(P_{sat}\cdot\tau\right)}A_y - \frac{i}{2}\beta_2\cdot\frac{\partial^2 A_y}{\partial t^2} \quad (2)$$

where A_x, A_y are the orthogonal components of the field envelope, z is a longitudinal coordinate, t – time, $\gamma = 4.7 \times 10^{-5}$ $(\text{cm}\cdot\text{W})^{-1}$, $\beta_2 = 23$ ps^2/km – non-linear and dispersion coefficients, $g_0 = 540$ dB/km – unsaturated gain coefficient, $P_{sat} = 52$ mW – saturation power for the active fiber, $\tau = 48$ ns – duration of cavity round trip. As in [13,14], we integrated Eqs. (1) and (2) over 10^4 round-trips using white noise as the initial condition for the first iteration. Since NPE mode-locked lasers may produce pulses with considerably different spectral width, we choose for our study a thin non-linear crystal with phase matching bandwidth wider than the spectral bandwidth of all considered pulses. It should be emphasized that it is the influence of phase fluctuations of double-scale pulses on SHG efficiency that we aim to determine, rather than the absolute values of SHG efficiency. In SHG modeling we follow the

#199337 - $15.00 USD Received 14 Oct 2013; revised 6 Dec 2013; accepted 3 Jan 2014; published 10 Jan 2014

approach described in [29]. Once the fundamental wave spectrum consists of N equally spaced modes ω_{1j}, the second harmonic (SH) should have $2N - 1$ modes with the same frequency step $\Delta\omega$. A schematic of elementary processes of frequency doubling and mixing is shown in Fig. 1(b) for $N = 3$ modes. Direct frequency doubling processes are marked with solid bold lines and frequency sum mixing processes, with dashed ones. Complex mode amplitudes A_{in} (n-th mode of i-th harmonic) are governed by Eq. (3):

$$\frac{\partial A_{2n}}{\partial z} + \frac{1}{u}\frac{\partial A_{2n}}{\partial t} = -i\sigma_2 \sum_{j+k=n+1} A_{1j} A_{1k} \tag{3}$$

where u is the group velocity, σ_2 is the nonlinear coefficient. Terms with $j = k$ in Eq. (3) correspond to direct frequency doubling and those with $j \neq k$, to sum frequency mixing. In the case of thin non-linear crystal, one can neglect dispersion and first harmonic depletion and take A_{1i} = const. Assuming $A_{2n} = 0$ at $z = 0$, let's integrate Eq. (3) from 0 to L and divide total SH power $I_{2n} = \Sigma|A_{2n}|^2$ by $(\sigma_2 L P_1)^2$, where P_1 is the first harmonic sum power:

$$\zeta = \left(\sum_n \left| \sum_{j+k=n+1} A_{1j} A_{1k} \right|^2 \right) \cdot \left(\sum_j \left| A_{1j} \right|^2 \right)^{-2} \tag{4}$$

In other words, ζ is the SHG relative efficiency which equals to the ratio of two SH powers, of which the first is obtained when the non-linear crystal is pumped by a double-scale laser pulse with given mode amplitudes A_{1j} and the second is generated with the use of single-mode monochromatic pumping of the same power $P_1 = \Sigma|A_{1j}|^2$. The dimensionless SHG relative efficiency ζ does not depend on power and thickness of the thin non-linear crystal but is sensitive to mode correlations and fluctuations, thus allowing us to easily compare different lasing regimes from the viewpoint of efficiency of non-linear frequency. To achieve this goal, we will simulate generation of double-scale pulses by numerically integrating Eqs. (1) and (2) and averaging SHG relative efficiency (4) over multiple cavity round-trips.

3. Results of modeling

First of all, we select PC settings of the simulated laser in order to achieve a stable single-pulse (per round-trip) generation regime with conventional bell-shaped pulses, Π-shaped spectra and smooth phase [14]. If we adjust the settings of PC2, we can gradually tune the laser from the conventional lasing regime via intermediate one towards noise-like generation. Let's note that in order to obtain reliable and reproducible results in experiments it's better to use polarization controllers based on bulk elements (wave plates), however in theoretical treatment all types of polarization controllers provide polarization transformations according to unitary matrices thus allowing one to obtain the same results. The evolution of SHG relative efficiency ζ in the process of laser regime switching is shown in Fig. 2. While the laser operates in the conventional regime, ζ evolves gradually due to change of pulse duration, peak power and spectral width (green line in Fig. 2). When the laser falls into generation of double-scale pulses, ζ drops stepwise by several per cent and then continues to decrease due to emergence and growth of mode phase fluctuations (red line in Fig. 2). Note that for double-scale pulses, ζ is not constant and fluctuates over successive round-trips along with other pulse parameters [13,14], which is indicated in Fig. 2 with a grey band which half-width is equal to rms fluctuation amplitude of ζ. Let's also note that SHG relative efficiency is comparable for both types of pulses and varies by only about 15%. Of course, Fig. 2 shows the one-dimensional vicinity of only one point in generalized space of PC settings and thus should not be used to draw any conclusions about all possible lasing regimes. Preparation and analysis of similar plots for all possible points is a considerable challenge, therefore we propose to study different regimes through a statistical approach.

#199337 - $15.00 USD Received 14 Oct 2013; revised 6 Dec 2013; accepted 3 Jan 2014; published 10 Jan 2014

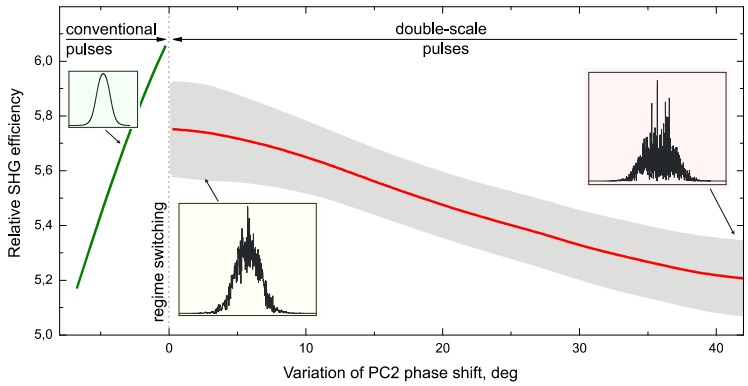

Fig. 2. Evolution of relative SHG efficiency (4) in the process of laser regime switching. Insets show laser pulses in different moments of gradual regime transition.

Let's choose PC settings in a random way and simulate lasing for each random realization during 10^4 cavity round-trips. If the laser starts to generate either conventional or double-scale pulses let's save the averaged (over successive round-trips) SHG relative efficiency ζ. If the laser fails to start pulse generation with random PC settings let's proceed to the next random PC settings without saving any data. Then let's plot accumulated values of ζ as a histogram (see Fig. 3) separately for conventional and double-scale pulses. Figure 3 shows resulting histograms obtained for 500 (16 700) realizations of conventional (double-scale) regimes. Note that discovered realizations of each of two key regimes differ in pulse energy, duration, bandwidth, etc. due to different PC settings. As it can be seen from Fig. 3, SHG relative efficiency may vary by an order of magnitude both for conventional and double-scale pulses, being a function of peak power, pulse and spectral width and shape and phase fluctuation level. However, the width of the ranges in which ζ varies as well as probability density functions (pdf) shown in Fig. 3 is pretty similar for conventional and double-scale pulses, despite the fact that the latter also demonstrate fluctuations in intensity and phase.

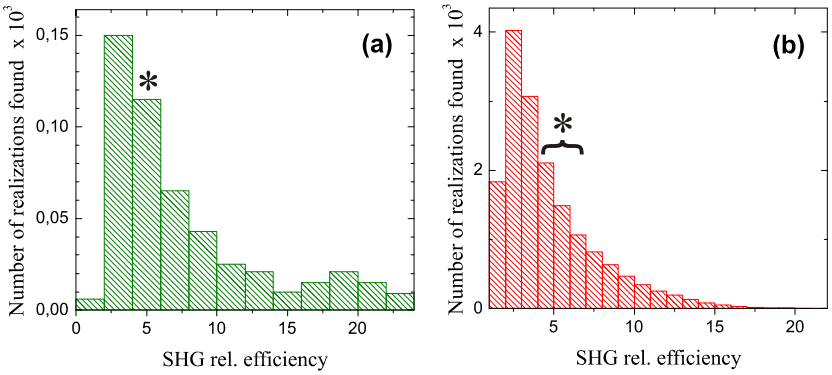

Fig. 3. Relative SHG efficiency histograms for (a) conventional and (b) double-scale pulses for random PC settings. Asterisks show histogram bars that correspond to simulation results shown in Fig. 2.

Simulation results allow us to examine the relation between SHG efficiency ζ and pulse parameters, such as duration T_{rms} and spectral width Ω_{rms}, which are essential for optimization of SHG efficiency. In this manner we found a strong anti-correlation between ζ and rms pulse duration T_{rms} with Pearson correlation coefficient $\rho(\zeta, 1/T_{rms}) = 0.97$, whereas correlation between ζ and spectral width Ω_{rms} is much smaller: $\rho(\zeta, \Omega_{rms}) = 0.45$. Another quite strong correlation is $\rho(\zeta, \Omega_{rms}/T_{rms}) = 0.94$. Diagrams in Fig. 4 illustrate correlation between ζ and

#199337 - $15.00 USD Received 14 Oct 2013; revised 6 Dec 2013; accepted 3 Jan 2014; published 10 Jan 2014

T_{rms} (Fig. 4(a)) and much weaker correlation between ζ and Ω_{rms}. (Fig. 4(b)). Each red (green) point on these diagrams corresponds to one realization of double-scale (conventional) pulse generation regime discovered in simulations. It can be seen that ζ is roughly inversely proportional to T_{rms} or, in other words, that ζ grows linearly with pulse peak power, as it should be for a second-order non-linear process. The correlation between ζ and spectral width Ω_{rms} can be expected since SHG efficiency is proportional to the number of mutually coherent modes [29]. One can also note in Fig. 4(a) that for any fixed pulse width T_{rms}, relative SHG efficiencies are comparable for both regimes, being slightly higher for double-scale pulses. Figure 4(b) suggests that double-scale pulses in general have wider spectrum compared to conventional pulses of the same efficiency of SHG.

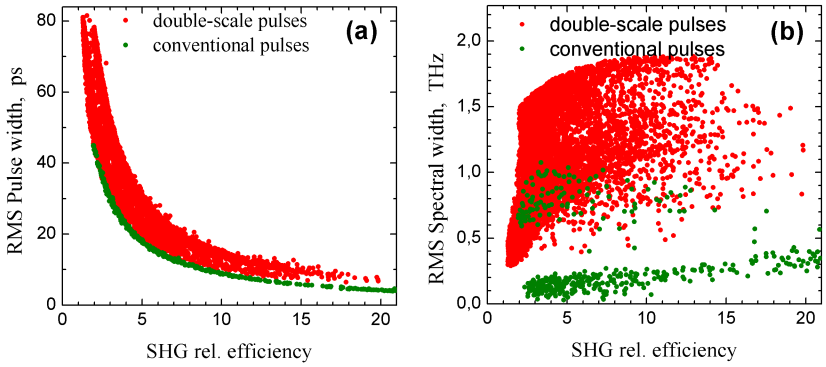

Fig. 4. Correlation between relative SHG efficiency and (a) rms pulse width, and (b) rms bandwidth of double-scale (red points) and conventional (green points) pulses.

4. Experiment

In order to verify the results of numerical simulation discussed above, we used a MOPA system with a master oscillator similar to the one shown in Fig. 1(a). The system operates at λ = 1100 nm, pulse repetition rate of 17 MHz, and average power up to 1.7 W. By tuning PC's, we obtained both conventional and double-scale pulses with duration of about 10 ps. To boost efficiency of the second harmonic generation, we used comparatively long (30 mm) non-linear LBO crystal in non-critical phase matching. The chosen type of phase matching ensured a relatively broad spectral acceptance bandwidth, which amounted to about 3 nm at the wavelength of 1100 nm. Nevertheless, this spectral acceptance bandwidth was substantially narrower than the spectrum width of both conventional and double-scale pulses (amounting to 15 nm). Therefore, only a part of the pulse spectrum was converted into the SH. A dichroic mirror was utilized to separate the SH radiation from the fundamental one. SHG efficiency was measured to be 4.7% for double-scale pulses and 3.2% for conventional pulses for the highest average pump power of 1.7 W. The experimentally observed efficiency values generally corroborate the modeling results in that the non-linear conversion efficiency for double-scale and conventional pulses may be of the same order of magnitude, and that for certain types of double-scale pulses, efficiency of their non-linear conversion may be higher.

5. Conclusion

By using numerical simulation based on non-linear Schrödinger equations, we investigated efficiency of second harmonic generation as an example of non-linear frequency conversion of double-scale pulses generated in a passively mode-locked fiber master oscillator. We found that SHG relative efficiency (i.e. efficiency for double-scale pulses divided by that for monochromatic pumping of the same power) for both double-scale pico-femtosecond and conventional picosecond laser pulses may vary by more than an order of magnitude depending on pulse peak power, duration and spectral width, which in turn are functions of

#199337 - $15.00 USD Received 14 Oct 2013; revised 6 Dec 2013; accepted 3 Jan 2014; published 10 Jan 2014

PC settings. Surprisingly, SHG relative efficiency for double-scale pulses was found to be slightly higher than that for conventional laser pulses of the same duration and energy, despite different level of intensity and phase fluctuations in these lasing regimes. In modeling, this result is related to higher peak powers and wider spectrum of double-scale pulses compared to that of conventional ones. In experiment, non-linear conversion efficiency of double-scale pulses also turned out to be higher, notwithstanding the fact that only 20% of spectrum of both types of pulses was converted into the second harmonic. The results of this work encourage further exploration of double-scale pulse applications since generation of such pulses is usually more environmentally stable and allows higher pulse energies.

Acknowledgments

This work was supported by the Marie-Curie International Exchange Scheme, Research Executive Agency Grant "TelaSens" No 269271; Grants of Ministry of Education and Science of the Russian Federation (agreement No. 14.B25.31.0003; project No. 01200907579; project No. ZN-004); Russian President grant MK-4683.2013.2.